Review of "Two different phytoplankton blooming mechanisms over the East China Sea during El-Niño decaying summers" by Lee et al.

Comment on egusphere-2024-3406 | Anonymous Referee #2:

Based on limited observations, previous studies suggested that in post-El Nino summers (JJA), increased runoff from the Yangtze River reduces salinity and increases Ch-a concentrations in the surface layer of the East China Sea (ECS). The present study extends the previous studies by using longer observations, suggesting that the western North Pacific anticyclone (WNPAC) in the lower troposphere during post-El Nino summers contributes to positive Ch-a anomalies in the ECS also through positive wind stress curl anomalies, which enhance upwelling of high nutrients from below the seasonal thermocline. The paper is generally well written and should be eventually published after addressing the following concerns.

Response: We thank referee #2 for encouraging and valuable comments on our manuscript. We have thoroughly addressed the feedback and revised the manuscript by fully incorporating the referee's suggestions.

Major comments.

1. The new mechanism of wind curl-induced upwelling is mostly based on a coarse-resolution ESM but the observational support is marginal. While observed Ch-a increase during post-El Nino summers is east of the Yangtze River estuary (Fig. 1a), positive wind curl anomalies are further to the south (Fig. 9b), almost entirely outside the ECS. The geographical discrepancy between Ch-a and wind curl anomalies needs to be reconciled. Just a thought: rainfall over eastern China takes a while to reach the coast and affects ECS Ch-a. Could this delay be important? Also there are many big reservoirs along the Yangtze River and water is being diverted from the river. Are these human controls important for discharges at the estuary?

Response: We indeed thank the referee's valuable comments and suggestions. We have thoroughly revised the manuscript, completely reorganizing and rewriting it to emphasize the significance of our findings.

We have newly incorporated the contribution of nutrient supply through the TS to phytoplankton blooming in the ECS into the revised manuscript, as supported by several references (Huang et al., 2015; Chen et al., 2015; Zhang et al., 2015). Both observational data and model results reveal that nutrient transport through the TS into the ECS is intensified during El Niño decaying summers (Figure R1; we added Figure R1a as Figure 1d to the revised manuscript). This enhancement is driven by the intensification of southwesterly winds over the South China Sea (SCS), which is facilitated by the development of the Western North Pacific Anticyclone (WNPAC) during the El Niño decaying summers. We have added the following paragraph to the revised manuscript to describe the TS-transport-driven blooming mechanism based on the model results:

(L256-265): We also investigated the TS-transport-driven blooming mechanism, which is well known for its significant role in nutrient supply through the TS. We analyzed the meridional PO4 transport by comparing two groups as the same as Fig. 5, and found remarkably distinct differences between them (Figure 6a-c). Notably, within the TS, a strong positive (negative) signal was identified in the SB (NB) group. For the SB group, the nutrient flux exhibits a significant positive signal reaching the target region, potentially supplying large amount of nutrients and making a substantial contribution to SCHL blooming in the ECS region. Furthermore, a positive correlation of 0.68—higher than the runoff-driven mechanism—was identified between the anomalous SCHL blooming magnitude in the target region and the meridional PO4 transport index indicated by the blue diagonal box in the TS region (Figure. 6d). This underscores the critical role of the TS-transport-driven mechanism in fostering nutrient into the ECS region.

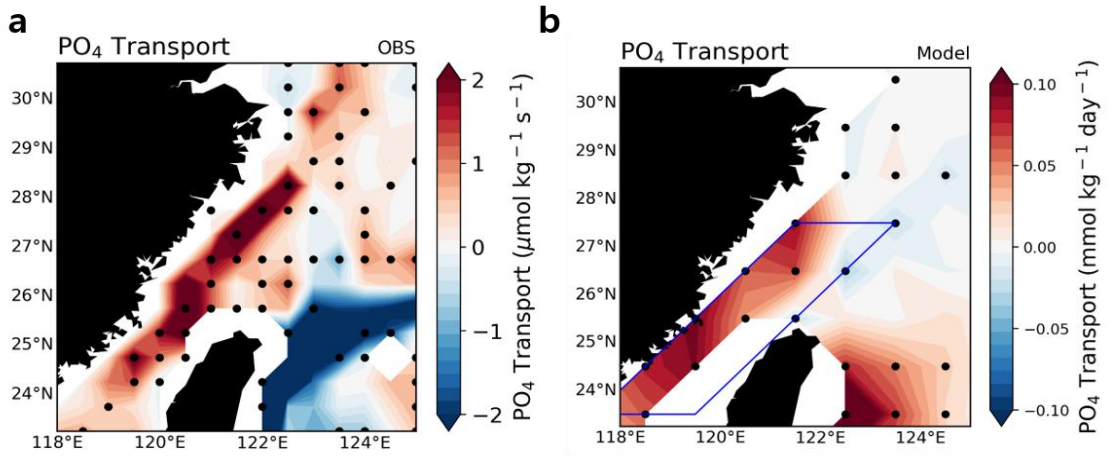

Figure R1. Composite map of meridional PO_4 transport anomalies during El Niño decaying summer season in the Taiwan Strait (TS) for all El Niño cases in observations (Left Panel) and model results (Right Panel). All the black dots where the responses are statistically significant at the 90% (in observations) and 95% (in model results) confidence level, determined using the bootstrap method.

Furthermore, our model results also showed that meridional phosphate (PO_4) transport through the TS contributes more significantly to SCHL in the ECS compared to runoff-driven mechanism (Figure R2; we added the Figure R2b as Figure 6d to the revised manuscript). Additionally, in the Strong Blooming (SB) group, the meridional PO_4 transport through the TS was stronger (Figure R3; we added the Figure R3 to the revised manuscript as Figures 6a–c).

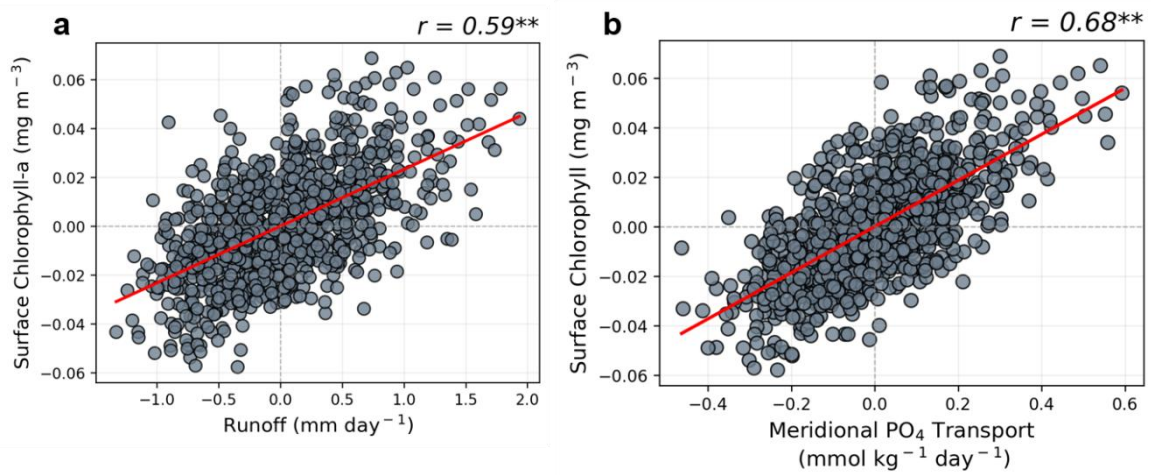

Figure R2. The relationship between area-averaged runoff and SCHL anomalies over the target region (Figure R3a), and the relationship between area-averaged meridional PO_4 transport and SCHL anomalies over the target region (Figure R3b).

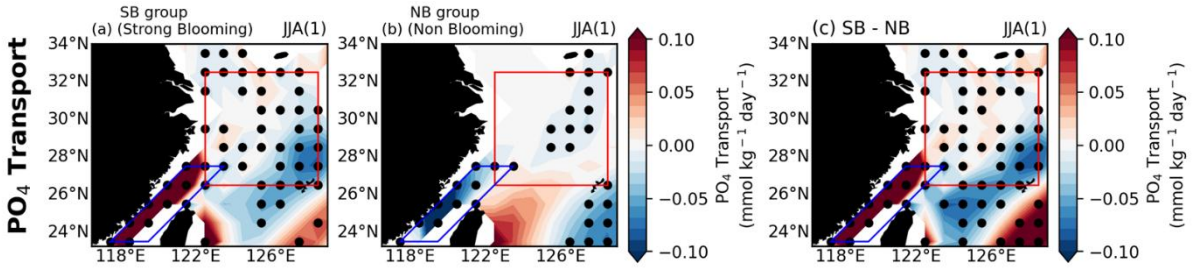

Figure R3. Composite maps of meridional PO_4 transport anomalies during El Niño decaying summer for Strong Blooming group (Figure R4a), Non-Blooming group (Figure R4b) and the difference between the two groups (Figure R4c).

The ESM we employed is indeed a low-resolution model with a 1˚ grid. We also agree with the reviewer that the high-resolution model can reflect more realistic contributions of the various phenomena. However, since the wind stress curl pattern exhibits a somewhat large-scale pattern, we believe the coarse resolution model is capable of simulating our main mechanisms. Satellite observations indicate that anomalous SCHL blooming regions in the East China Sea (ECS) are strongly concentrated around the Yangtze River Estuary (YRE) during El Niño decaying summers, with weaker diagonal signals extending northeast from Taiwan to the Korea

Strait. The observed positive wind stress curl anomalies are widespread, covering areas from the YRE through the Taiwan Strait and extending to the Luzon Strait. In the East Asian Marginal Seas, including the ECS, are featured by a northward current from the TS and Kuroshio Current. Therefore, the climatological northward flow of the Kuroshio Current and the currents passing through the TS during summer enable the transport of anomalous upwelled nutrients due to the widespread cyclonic wind stress curl across the ECS and even to the Korea Strait (Figure R4).

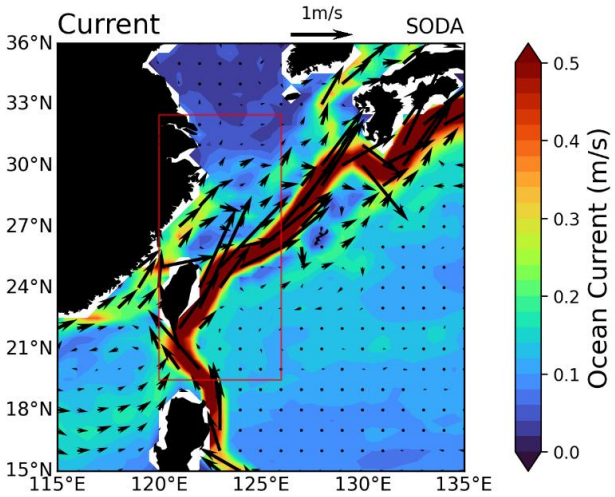

Figure R4. Climatological oceanic current over the East Asian Marginal Seas. Vectors indicate the oceanic current and shading shows the oceanic current speed. The red box indicates the Wind Stress Curl index as selected in the manuscript.

Additionally, in the revised manuscript, we assessed the relative contributions of three mechanisms using a regression method instead of the joint-composite analyses (Figure R5, Table R1; We added Figure R5 and Table R1 as Figure 9 and Table 1 in the manuscript respectively). We normalized all variables and conducted multiple regression for three mechanism indices at each grid point of SCHL anomalies across the target region. And, we quantified the relative contributions of three mechanisms by multiplying the linear regression coefficients between the Nino3.4 index and each mechanism index by their multiple regression coefficients respectively (Eq. 1; We added it as Eq. 4 in the manuscript).

The results indicate that both the Runoff- and the TS-transport-driven mechanism have the most significant contributions to the intensity of SCHL blooming in the target region. Although the Ekman Upwelling-driven mechanism exhibits a lower contribution compared to the others, it still exerts a meaningful influence on about half of the other mechanisms. Spatially, the Runoff-driven mechanism primarily affects the central area of the target region (Figure R5a), while the TS-transport-driven mechanism plays a major role along a southwest-northeast diagonally (Figure R5b). In contrast, the Ekman Upwelling-driven mechanism uniformly influences the overall target region (Figure R5c). Especially, the runoff- and the TS-transport-driven mechanism contribute similarly to the SCHL blooming intensity in the target region. Although the Ekman upwelling-driven mechanism accounts for approximately 40 to 47% of the others, it still exerts a significant influence (Table R1). Consequently, we have replaced the paragraph that calculated the relative contribution for each mechanism from the joint-composite analyses previously we used to the regression method as follows:

(L313-349): So far, we have conducted a comprehensive evaluation and analysis of the complex mechanisms driving phytoplankton blooms in the ECS during the summers following the decaying phase of El Niño events. In addition to the runoff- and TS-transport-driven mechanisms suggested in previous studies, we introduced the Ekman upwelling-driven blooming mechanism. Subsequently, we quantified the relative contributions of these three mechanisms based on regression methods using (Eq. 4) as follows:

$$\frac{dChl}{dNino3.4}(\alpha) = \frac{\partial Chl}{\partial Runoff} \times \frac{dRunoff}{dNino3.4} + \frac{\partial Chl}{\partial TS-transport} \times \frac{dTS-transport}{dNino3.4} + \frac{\partial Chl}{\partial Ekman-Upwelling} \times \frac{dEkman-Upwelling}{dNino3.4} + residual \quad (4)$$

Firstly, we normalized all variables and conducted the multiple regression with respect to SCHL index in the target region as the dependent variable and three mechanism indices as independent variables. Secondly, we calculated each term by multiplying the linear regreesion coefficient between Nino3.4 index and each mechanism index by the corresponding multiple regression coefficient for each mechanism index. The combined effects of the three mechanisms and the residual term collectively account for the variation of the SCHL index in

the ECS region with respect to the El Niño events. Therefore, each term indicates how changes in three mechanism induced by ENSO cycle (as indicated by the Nino3.4 index) affect on phytoplankton blooms in the ECS region. The results show the effect of runoff-driven mechanism and the TS-transport mechanisms to SCHL blooming intensity in the target region are comparable (Table 1). In the case of the Ekman upwelling mechanism, it accounts for about 40% to 47% of contributions comapred to the other two mechanisms, yet still exerts a meaningful influence as well.

Table R1. Relative contributions of three mechanisms to SCHL blooming in the target region.

	α	Runoff	TS-transport	Ekman Upwelling
Contribution	0.511	0.152	0.138	0.065

Additionally, we identified their spatial contributions to further elucidate the effects of each mechanism within the target region (Figure 9). We conducted multiple regression for three mechanism indices at each grid point of SCHL anomalies across the target region. Following the same way examined above, we calculated the spatial contributions by multiplying the linear regression coefficents of each mechanism with repsect to the Nino3.4 index. The results showed that the runoff-driven mechanism exhibited the strongest contribution at the center of the target region, driven by direct riverine nutrient inflow (though the model doesn't simulate P input) and nutrient supply through buoyancy upwelling induced by river discharge (Figure 9a). In contrast, the TS-transport-driven mechanism significantly contributes along a southwest-northeast diagonal direction, aligning with nutrient transport via the TS from the SCS (Figure 9b). Additionally, the newly proposed Ekman upwelling-driven mechanism, while relatively lower in overall contribution, shows significant and uniformly distributed impacts across the target region (Figure 9c). These results suggest that all mechanisms can affect comprehensively to induce phytoplankton blooms in the ECS during the following summers of the decaying phase of El Niño events. Therefore, considering all mechanisms is essential for accurately predicting the intensity of phytoplankton blooms.

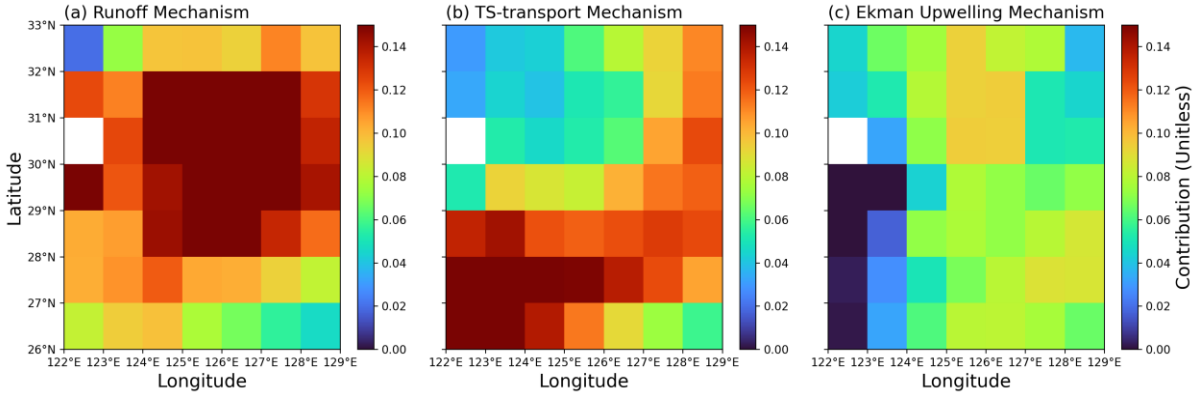

Figure R5. Relative contributions of three mechanisms to SCHL blooming in the target region during summers following the decaying phase of El Niño events **(a)** Runoff-driven mechanism **(b)** TS-transport-driven mechanism **(c)** Ekman upwelling-driven mechanism.

Our modelling analyses suggest that the upwelling-driven mechanism operates as an supplemental mechanism, therefore, even if the location of maximum upwelling does not always coincide with areas of maximum phytoplankton blooms.

In addition. we investigated the lagged relationship between summer SCHL in the target region and monthly precipitation over the eastern China to analyze the time delay of the effect of rainfall on the SCHL. Our results indicate that summer season SCHL in the ECS region is most strongly correlated with concurrent summer precipitation (Figure R6). In particular, the July–August precipitation in the observations and the June–July precipitation in the model each showed the highest correlation with summer SCHL. Moreover, for both the observations and the model, summer SCHL exhibited the highest correlation with JJA seasonal precipitation. Therefore, we believe that time delay in the impact of rainfall on SCHL in the ECS region does not significantly compromise the validity of our study.

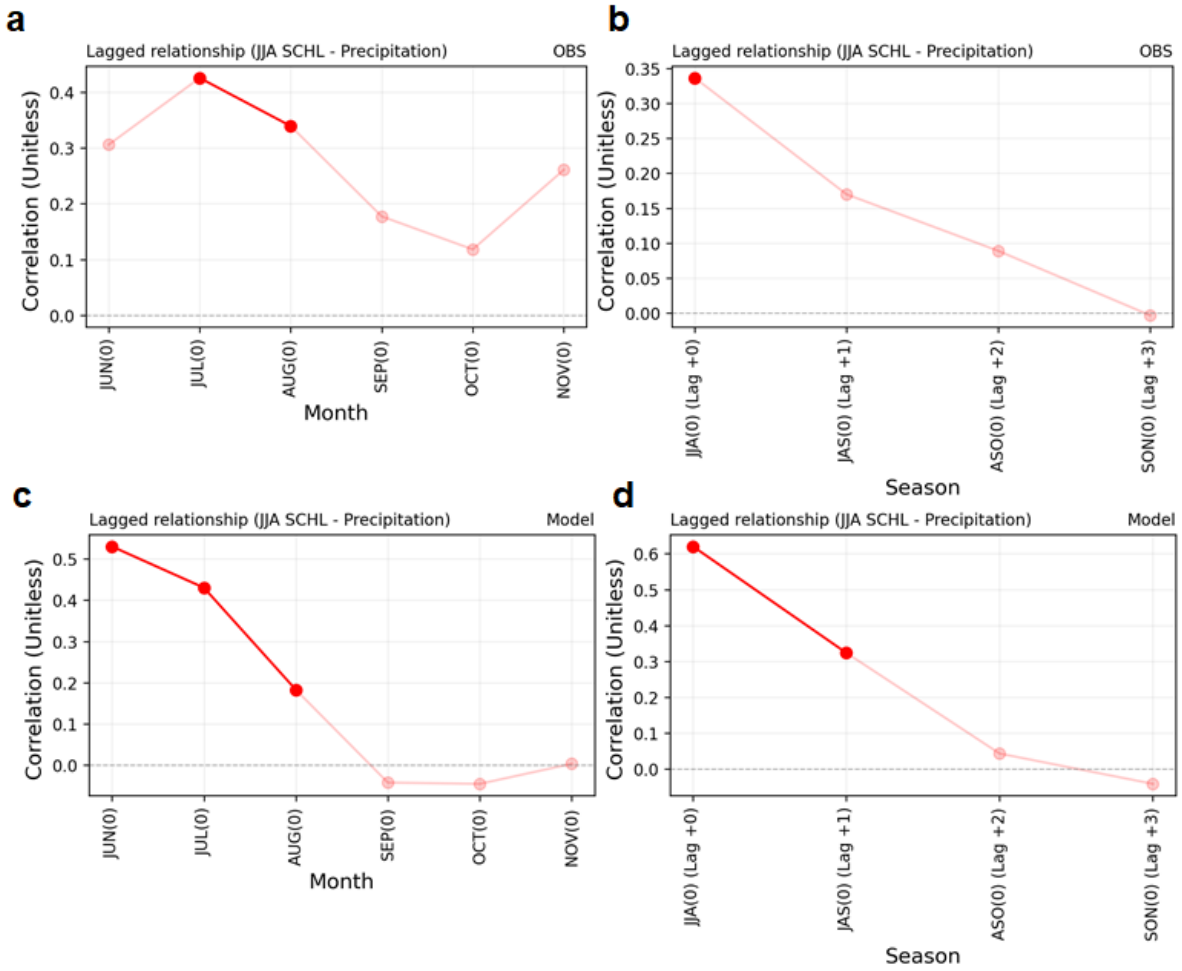

Figure R6. The plot shows the lagged relationship between precipitation during summer season (June-July-August; JJA) and the surface Chlorophyll-a (SCHL) in the target region of both **(a-b)** observations and **(c-d)** model. **(a)** The plot shows 6 month lagged relationship between summer season SCHL and monthly precipitation in the eastern China (Observations: 30.5˚N-32.5˚N / 114˚E-119˚E; Model: 27.5˚N-33.5˚N / 117.5˚E-124.5˚E, which is broader than observations) from June (0) to the November (0). **(b)** The plot shows the lagged relationship between the averaged summer season SCHL and the 3-month averaged precipitation from JJA (0) to SON (0). **(c-d)** As same as Fig. R6a-b, but the case of model results. The deeper red colors indicate that the p-value is below 0.1 (0.05), signifying statistical significance at the 90% (95%) confidence level for observations (model).

Indeed, in terms of anthropogenic impacts, the three Gorges Dam (TGD), located on the Yangtze River, has a substantial impact on the volume of river discharge flowing into the ECS. Increased water storage of the TGD leads to a reduction in river

discharge into the ECS, which in turn causes ecological changes such as shifts in chlorophyll-a and other marine ecosystem components (Jiao et al., 2007).

Furthermore, we have added the description that the runoff-driven mechanism encompasses nutrient input resulting from the entrainment of subsurface waters via buoyancy upwelling by following another referee's comment as follows:

(L139-145): In addition to the direct riverine nutrient input, enhanced river discharge can facilitate nutrients to the ECS region through buoyancy upwelling (Chen, 2008; Chen et al., 2003; Chen, 2000; Hill, 1998). When the out-flowing river plume becomes more substantial than the incoming river discharge, subsurface waters are readily upwelled to preserve the water balance. Consequently, the nutrient-rich Kuroshio subsurface waters ascend along the ECS shelf edge, providing essential nutrients. This buoyancy-driven upwelling occurs independently of wind conditions, driven primarily by the physical properties of the subsurface waters in response to the intensified river outflow.

(L170-174): Although the GFDL-CM2.1 ESM does not simulate P inputs from riverine inflows, it does account for P supply through the dynamic ascent of subsurface waters driven by buoyancy upwelling resulting from river discharge. Therefore, beyond analyses based on observational and reanalysis data, long-term model simulations enable us to comprehensively understand the phytoplankton blooming mechanisms in the ECS during the following summers of El Niño events.

We also have revised the title of the manuscript to **"Phytoplankton Blooming Mechanisms over the East China Sea during El Niño Decaying Summers"** to better reflect the scope and findings of our study.

Therefore, the extensively revised manuscript offers a more comprehensive understanding of the mechanisms driving phytoplankton blooming in the ECS during El Niño decaying summers, improving the previous manuscript.

2. ENSO is but one driver, but the WNPAC is an intrinsic mode of Asian summer monsoon variability and could be active in non-ENSO summers (P. Zhang et al. 2024, *JC*). The super-active Meiyu season in 2020 is a recent example (Z.Q. Zhou et al. 2021, *PNAS*). Could this explain the discrepancy between Figs. 1a and 9b?

Response: We appreciate the referee's suggestion regarding the mechanisms behind anomalous SCHL blooming that occur during Non-ENSO summers. Indeed, as the 2020 Super-active Meiyu season took place without considerable ENSO events (Figure R7). Specifically, the anomalous SCHL bloom intensity in 2020 (0.124 mg m^{-3}) is weaker than the average bloom intensity during El Niño periods (0.174 mg m^{-3}), despite experiencing the highest precipitation since 1961 and the consequent substantial river discharge (Zhou et al., 2021).

This finding indicates that SCHL blooming in the ECS is likely driven by a combination of several mechanisms. In addition to enhanced river discharge, nutrient transport through the TS and the supply of upwelled nutrients from sub-surface layer to the ECS via ocean currents—facilitated by a broad positive wind stress curl extending from the Yangtze River to the Luzon Strait—also play significant roles during the decaying summer season of El Niño.

Therefore, our study reveals that the upwelling-driven mechanism can play an additional role in phytoplankton blooming within the ECS with other mechanisms (runoff-driven and TS-transport-driven). The contributions of the runoff-driven and TS-transport-driven mechanisms to blooming are greater, thus, there may be a spatial discrepancy between the regions exhibiting the most intense anomalous surface chlorophyll-a (SCHL) blooms and the areas where upwelling occurs.

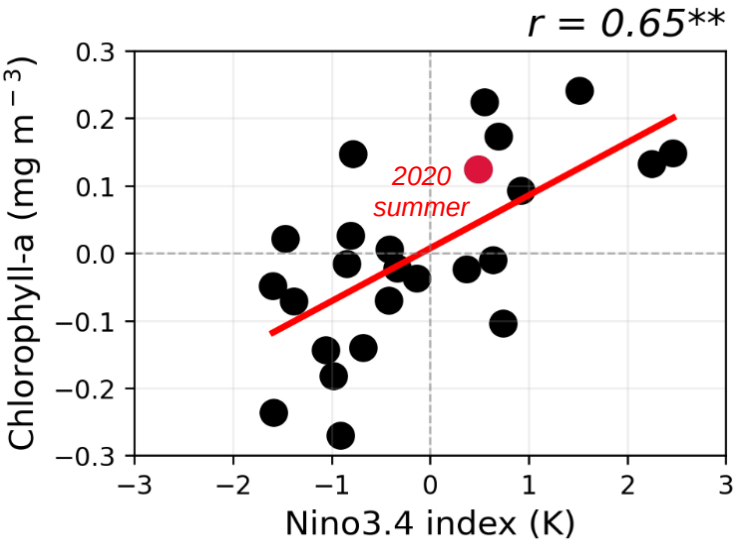

Figure R7. As same as the Figure 1b in revised manuscript, and the red circle indicates the case of 2020 supter-active Meiyu summer season.

Minor comments

1. The discussion of WNPAC dynamics is quite dated (L235-240, L386-394). See Xie et al. (2016, Adv Atmos Sci) and Chowdary et al. (2019, Current Clim Change Reps) for recent reviews.

Response: Thanks for suggesting the papers**.** We cited the references in the revised manuscript.

2. Regarding the global warming effect on WNPAC (L383-386), a CMIP6 analysis suggests that ENSO-induced variability does not change much but ENSO-unrelated variability intensifies with warming (C.Y. Wang et al. 2023, JC). This would imply a weakened ENSO effect on ECS Ch-a.

Response: We have incorporated the references in the revised manuscript

3. The writing is overall good but please check English grammar. L21: add “the” in front of “East China Sea”. L35: add “The” in front of “Western North.”

Response: Corrected.

Reference

Chen, C. T. A., Yeh, Y. T., Chen, Y. C., and Huang, T. H.: Seasonal and ENSO-related interannual variability of subsurface fronts separating West Philippine Sea waters from South China Sea waters near the Luzon Strait, Deep. Res. Part I Oceanogr. Res. Pap., 103, 13–23, https://doi.org/10.1016/j.dsr.2015.05.002, 2015.

Huang, T. H., Chen, C. T. A., Zhang, W. Z., and Zhuang, X. F.: Varying intensity of Kuroshio intrusion into Southeast Taiwan Strait during ENSO events, Cont. Shelf Res., 103, 79–87, https://doi.org/10.1016/j.csr.2015.04.021, 2015.

Jiao, N., Zhang, Y., Zeng, Y., Gardner, W. D., Mishonov, A. V., Richardson, M. J., Hong, N., Pan, D., Yan, X. H., Jo, Y. H., Chen, C. T. A., Wang, P., Chen, Y., Hong, H., Bai, Y., Chen, X., Huang, B., Deng, H., Shi, Y., and Yang, D.: Ecological anomalies in the East China Sea: Impacts of the Three Gorges Dam?, Water Res., 41, 1287–1293, https://doi.org/10.1016/j.watres.2006.11.053, 2007.

Zhang, W., Zhuang, X., Chen, C. A., and Huang, T.: The impact of Kuroshio water on the source water of the southeastern Taiwan Strait: numerical results, Acta Oceanol. Sin., 34, 23–34, https://doi.org/10.1007/s13131-015-0720-x, 2015.

Zhou, Z., Xie, S., and Zhang, R.: Historic Yangtze flooding of 2020 tied to extreme Indian Ocean conditions, 1–7, https://doi.org/10.1073/pnas.2022255118, 2021.